SPACE TELESCOPE SCIENCE INSTITUTE
Operated for NASA by AURA

Instrument Science Report WFC3 2001-012

Characterization of the UV PSF for WFC3

M. Stiavelli
June 27, 2001

ABSTRACT

The aim of this ISR is to document the design choices leading to the filter specifications adopted for WFC3. We also show the expected PSF in the UV filters, their enclosed energy and sharpness.

1. Introduction

The optical performance of the WFC3 UVIS channel optics is specified at 2500 A. We have verified that the instrument optical design does indeed satisfy the CEI Specification at this wavelength. The instrument will be operated without refocussing for each change of filter, therefore - for a constant equivalent optical thickness for all the filters - the PSF quality would rapidly degrade at wavelengths shorter than 3500 A because of the presence of refractive components in the instrument design (two camera head windows and the filter). The aim of this ISR is to describe this degradation, and show how it has been compensated by suitably specifying the optical thickness of the UV filters.

Our modelling methods will be presented in Section 2. The encircled energy variation across the field and its impact on the instrument sensitivity in the uncorrected case will be presented in Section 3. Section 4 analyses the performance for the instrument. It is easy to see that by specifying a lower effective thickness for the UV filter one can compensate for the higher effective thickness of the camera head windows and obtain confocality across the wavelength range of the instrument. In principle this solution corrects only for the filter central wavelength. We will discuss how the performance remains acceptable for the broadest filters. Our conclusions are drawn in Section 5.

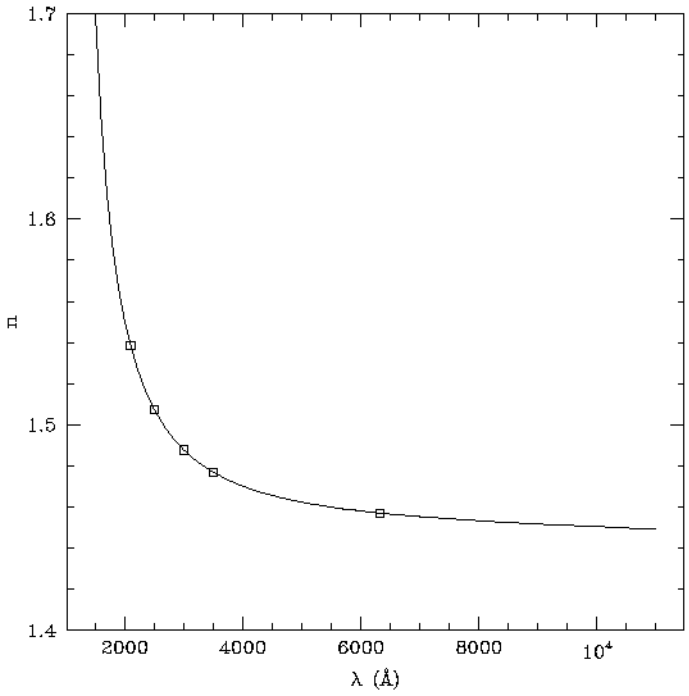

Figure 1: The refractive index of fused silica as a function of wavelength. The curve has been computed using a model while the points reflect the values built into ZEMAX.

2. Modelling method

The optical design of WFC3 was made available to us by Ball as a set Code V prescriptions. Unfortunately, Code V is no longer available at STScI and therefore we had to convert these prescriptions from Code V to ZEMAX. J. Krist carried out this conversion. We checked that the refractive index for fused silica used in ZEMAX is in agreement with the values computed following Malitson (1962). Using ZEMAX analysis tools, the PSF and encircled energy were computed at various location in the field of view and for a variety of wavelengths. The PSFs were converted into fits images and sampled with the actual pixel size of the UVIS channel by using a Fortran program. The ZEMAX PSFs include all optical effects but do not include the pixel MTF which is added after pixelation. MTF is, at this stage, highly uncertain and it has been assumed to be identical to that of WFPC2 (see WFPC2 Instrument Handbook). Given this uncertainty we have analyzed both the PSF with and then one without MTF.

We have initially considered the properties of the monochromatic PSF at 2100 A. The use of a monochromatic PSF at that wavelength is representative of observations of blue sources through the bluest UV filters of WFC3. We first used a fixed filter optical thickness in order to study how serious the defocus would be and then repeated the analysis for the filters as they have been actually specified by requiring confocality.

In most of the analysis we have considered three specific locations: the center of the field of view, a corner of the inscribed square used to specify the optical quality of the instrument and a corner of the field of view. The corners that we have chosen are representative of the behavior as a function of field position. Most of the degradation is observed to occur outside the inscribed square. This is clearly illustrated in Figure 2 where we show the PSFs - obtained for a UV filter with the same optical thickness as the visible filters - at these three locations before pixel sampling and with the equivalent filter thickness of the visible filters. The PSF variation is not as large after pixelation and the effect is mostly that of producing a brighter limiting magnitude.

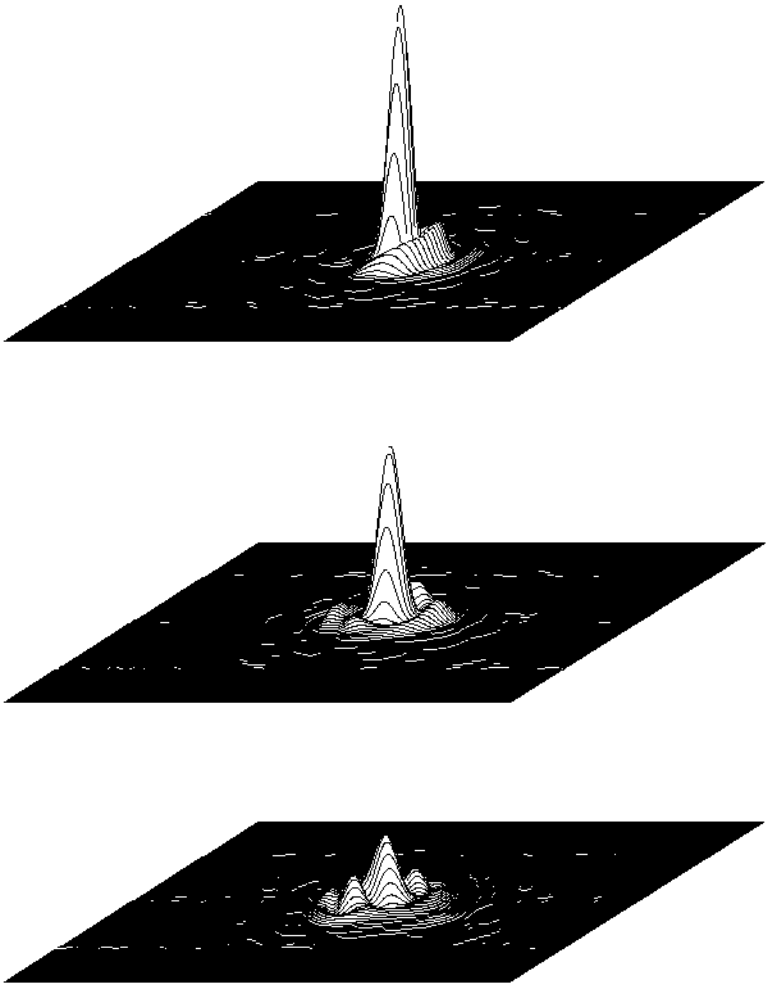

Figure 2: From top to bottom we plot for a non-confocal filter and before pixel sampling the 2100 A PSF at the center of the FOV, at the corner of he inscribed square and at the corner of the FOV. The size of each PSF is 150 μm, i.e., ~10 pixels or ~0.4 arcsec.

3. The case of uncompensated de-focus in the UV

The encircled energy for the PSF at 2100 A at the three locations shown in Figure 2 is plotted in Figure 3. The radius of 50 per cent encircled energy increases by more than a factor of two from the center of the field of view to the edge. The impact on performance would not be as large as suggested by the Figures 2 and 3 since the PSF is undersampled by a large factor. In Table 1 we list the values of the sharpness at the three locations with and without taking into account the effect of the pixel MTF. When computing sharpness, pixel sampling has been taken into account as described in Section 2.

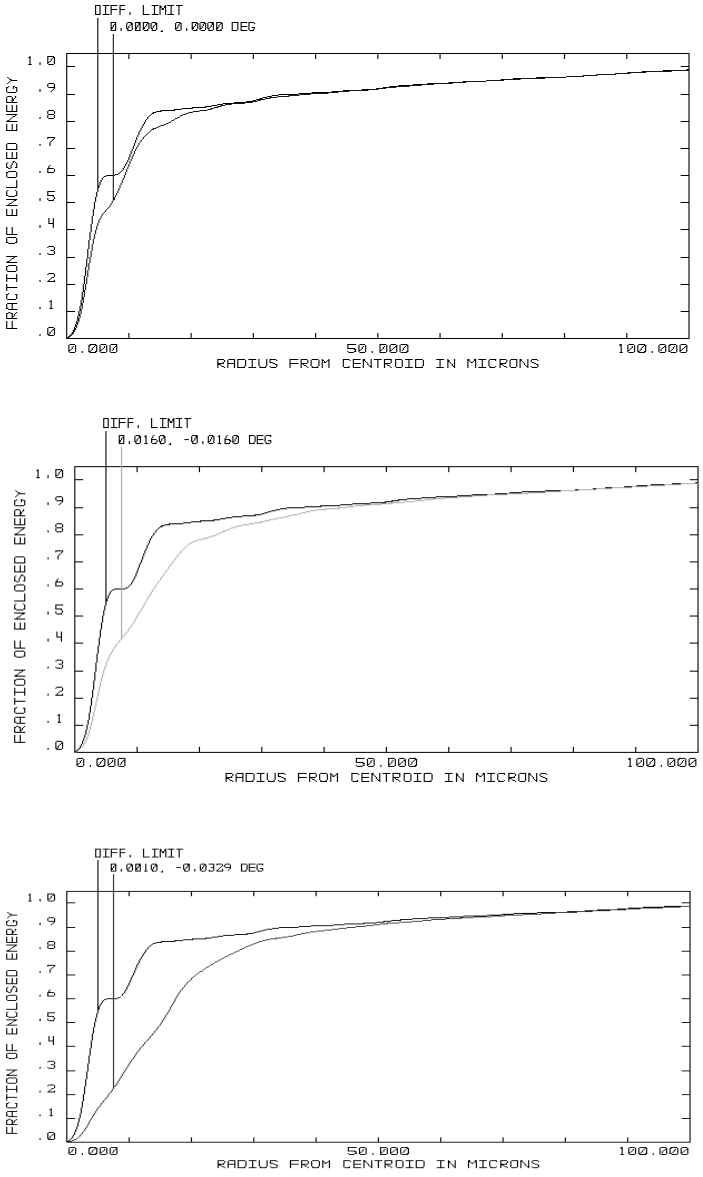

Figure 3: From top to bottom we plot the encircled energy before pixel sampling at 2100 A at the center of FOV, on the inscribed square and at the corner of the FOV. The pixel size is 15.5 μm. The diffraction limited encircled energy is also plotted for reference.

Location	Sharpness	Δ mag
Center - perfect MTF	0.322	0.00
Inscribed - perfect MTF	0.193	0.28
Edge - perfect MTF	0.101	0.63
Center - WFCP2 MTF	0.280	0.00
Inscribed - WFPC2 MTF	0.172	0.26
Edge - WFPC2 MTF	0.094	0.59

Table 1. Values of the Sharpness for PSF with non confocal filter computed at the three reference location after pixelation. We have considered the two cases of a perfect MTF or a WFPC2 style MTF. The last column gives the loss in depth due to the PSF degradation.

The sharpness of a PSF is essentially the inverse of the effective number of pixels collecting all the light and can be used to derive the S/N of images attainable with optimal extraction (see, e.g., WFPC2 Handbook). Therefore, a degradation in sharpness leads to a loss in depth. This is illustrated by the column Δmag in Table 1. Clearly, the MTF does not affect the result significantly. The loss in limiting magnitude would be modest within the inscribed square but it could exceed 0.5 magnitudes at the corners of the field of view.

4. How the filters compensate the UV defocus

The filters and the CCD camera head windows are the only refractive elements in WFC3 UVIS. Thus, the instrument would be in focus at all wavelengths if there was no camera head window and the filters had the same equivalent thickness. Since this walvength dependent focus is caused by the refractive elements one can specify the filters so as to compensate for the change of refractive index of the windows. This was done by Jennifer-Turner Valle at BASD and incorporated into the filter spec document.

The effective wavelengths and effective equivalent thicknesses of some of the UV filters are listed in Table 2. They have been computed according to the Malitson (1962) prescription for fused silica and to the equation specified in the JPL filter specifications. Note that for the F300X filter we have conservatively assumed confocality at 6000 A.

Below we discuss the resulting monochromatic PSF at 2100 A and the PSF in F218W, F225W, F275W and F300X corresponding to a flat spectrum source.

Name	λ_0 (A)	$\Delta\lambda_0$ (A)	n(λ_0)	thickness (mm)
F218W	2175	300	1.531	3.934
F225W	2250	500	1.524	4.056
F275W	2750	500	1.496	4.614
F336W	3375	550	1.479	4.980
F300X	6000	-	1.458	5.475
F280N	2798	42	1.494	4.651
F343N	3426	228	1.478	5.001

Table 2. UV filters that were considered for this study, their central wavelength, filter width, refractive index of fused silica at the central wavelength, and filter equivalent thickness (in mm of fused silica).

4.1 PSF at 2100A

Figure 4 shows the monochromatic PSF at 2100 A at the corner of the field of view obtained with the F225W filter. This PSF is a clear improvement over the one obtained without the confocality condition (bottom panel in Figure 2). The PSF through the F218W filter would be somewhat better because 2100 A is closer to the filter effective wavelength.

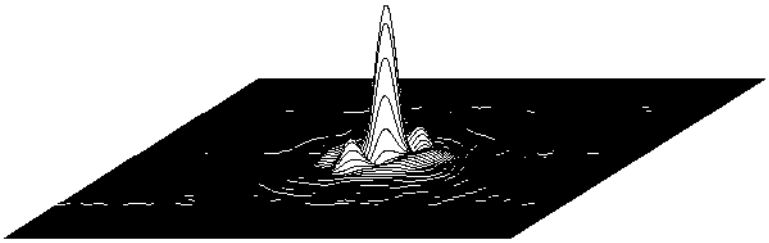

Figure 4: Monochromatic PSF at 2100 A at the corner position. This should be compared to the bottom panel of Figure 2.

4.2 Convolution of the filter bandwidth

We have computed for some of the UV filters the PSF corresponding to a flat input spectrum at a few locations in the field of view. Below we will discuss in detail the 4 cases where the PSF degradation and field dependence is the worst: F218W, F225W, F275W

and F300X (see Figures 5, 6, 7, and 8). The PSF size is specified in μm. The UVIS CCD pixel size is 15.5 μm.

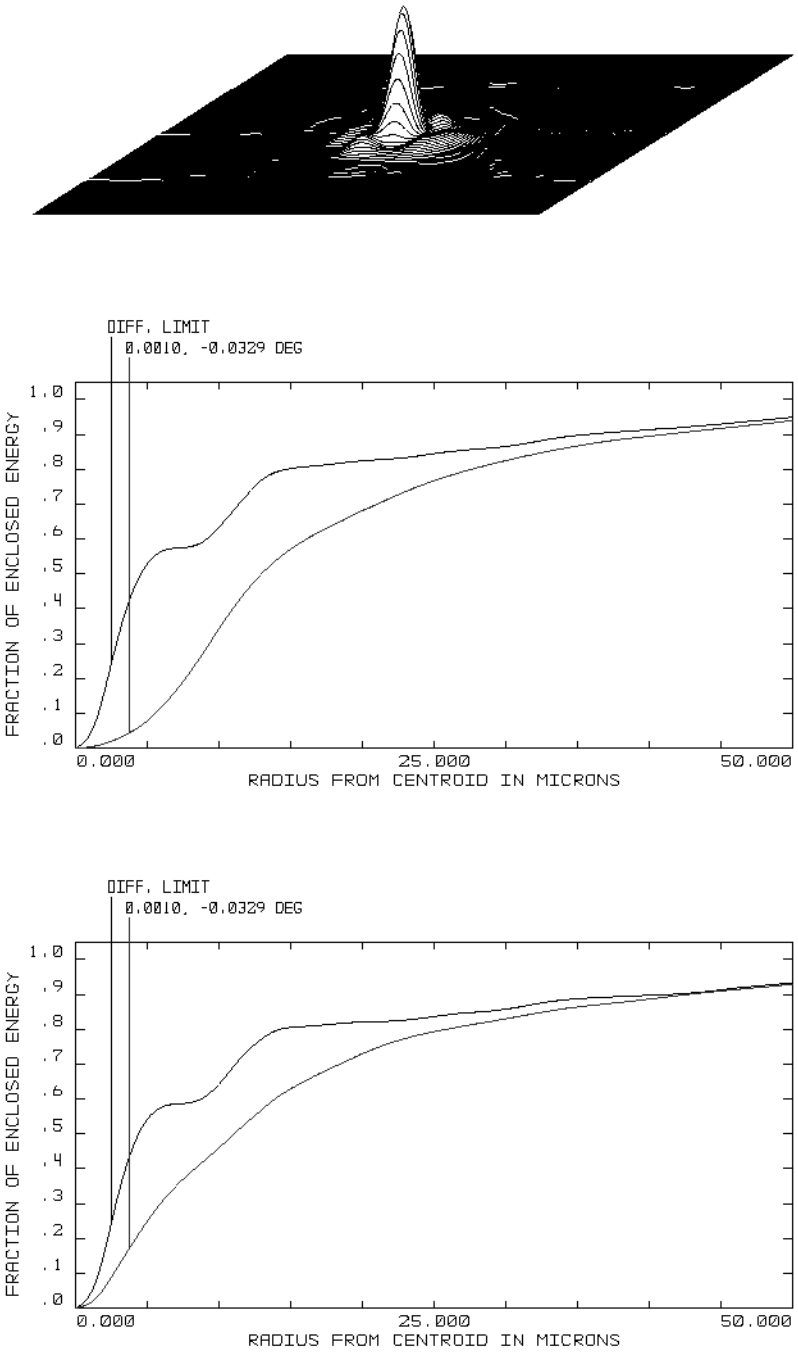

Figure 5: PSF for F218W at the edge of the field of view (top panel). Encircled energy for F218W at the edge of the field of view for a uniform spectrum (intermediate panel) and for a monochromatic source at the filter central wavelength (bottom panel).

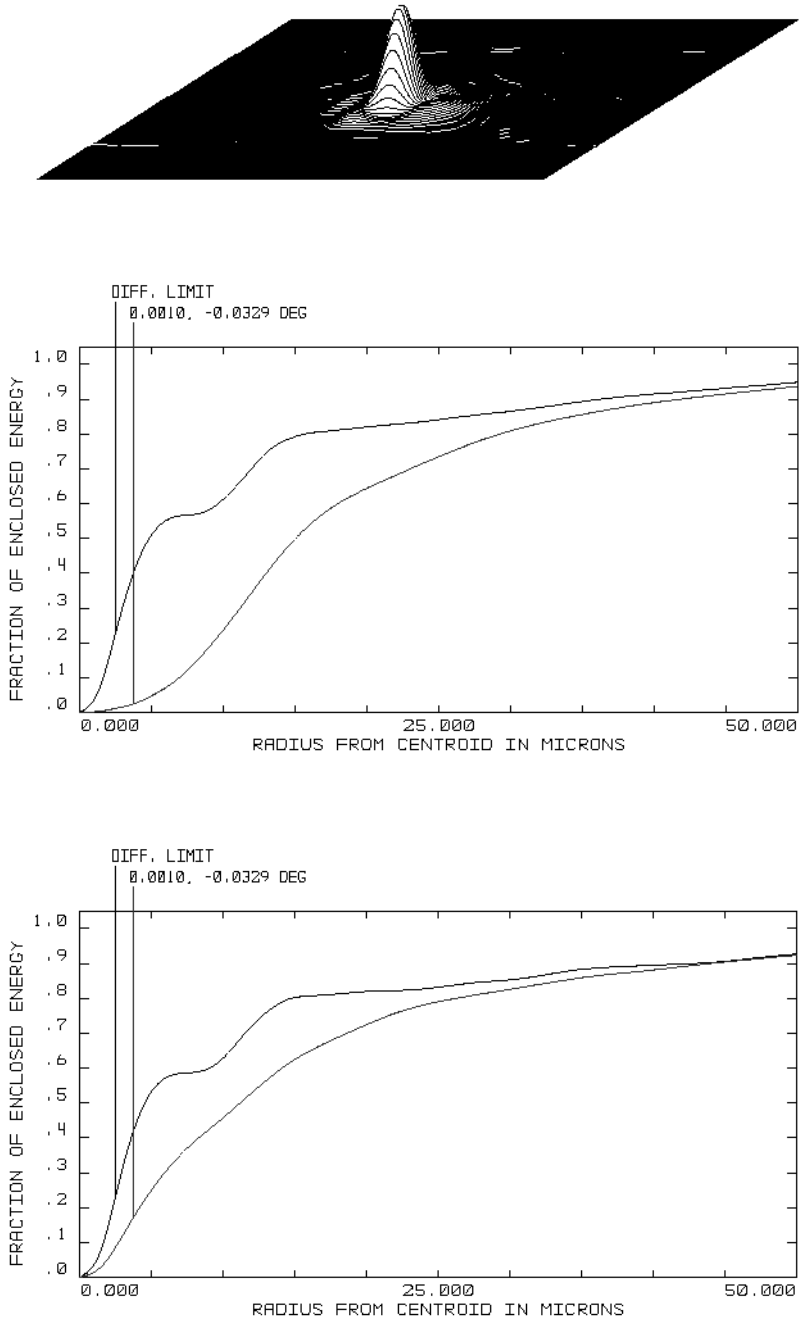

Figure 6: PSF for F225W at the edge of the field of view (top panel). Encircled energy for F225W at the edge of the field of view for a uniform spectrum (intermediate panel) and for a monochromatic source at the filter central wavelength (bottom panel).

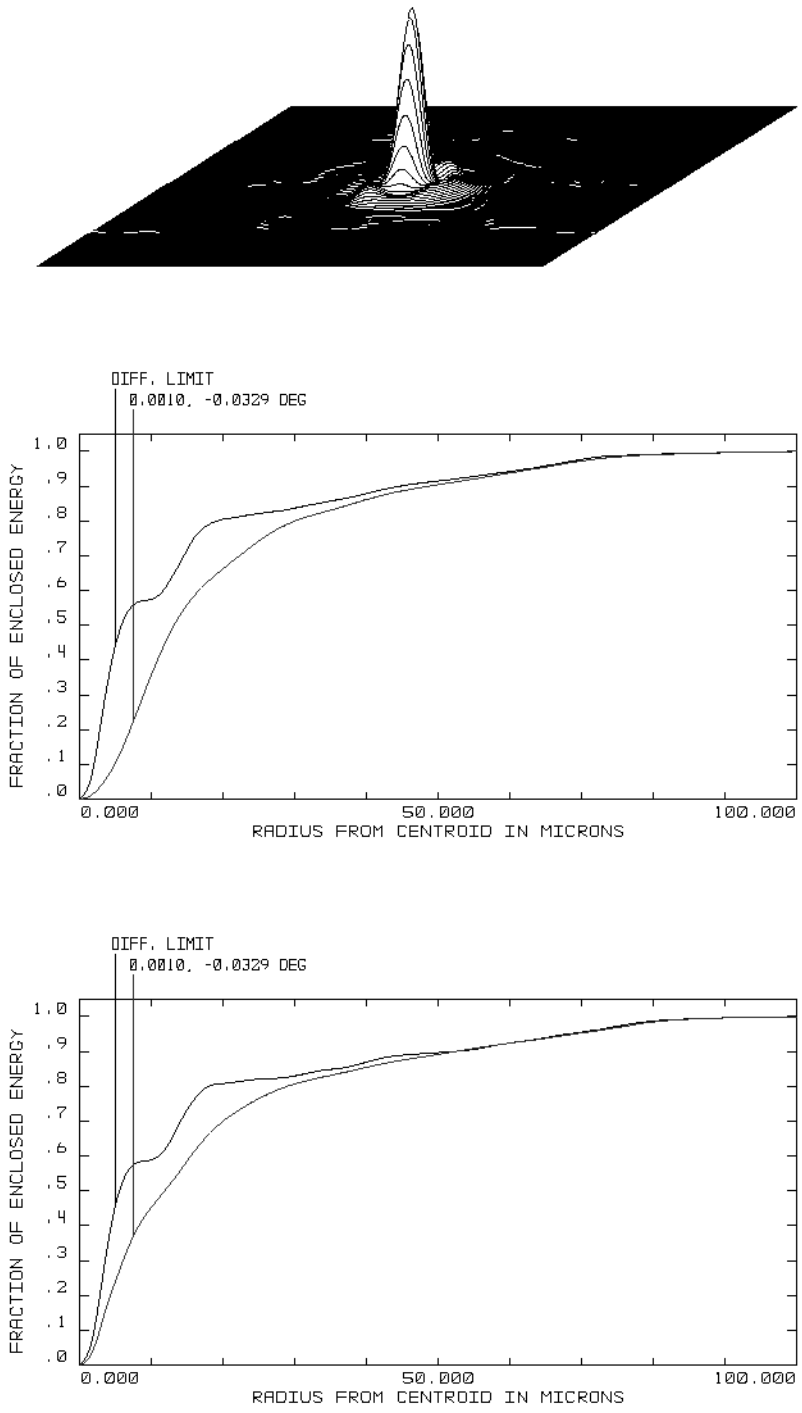

Figure 7: PSF for F275W at the edge of the field of view (top panel). Encircled energy for F275W at the edge of the field of view for a uniform spectrum (intermediate panel) and for a monochromatic source at the filter central wavelength (bottom panel)

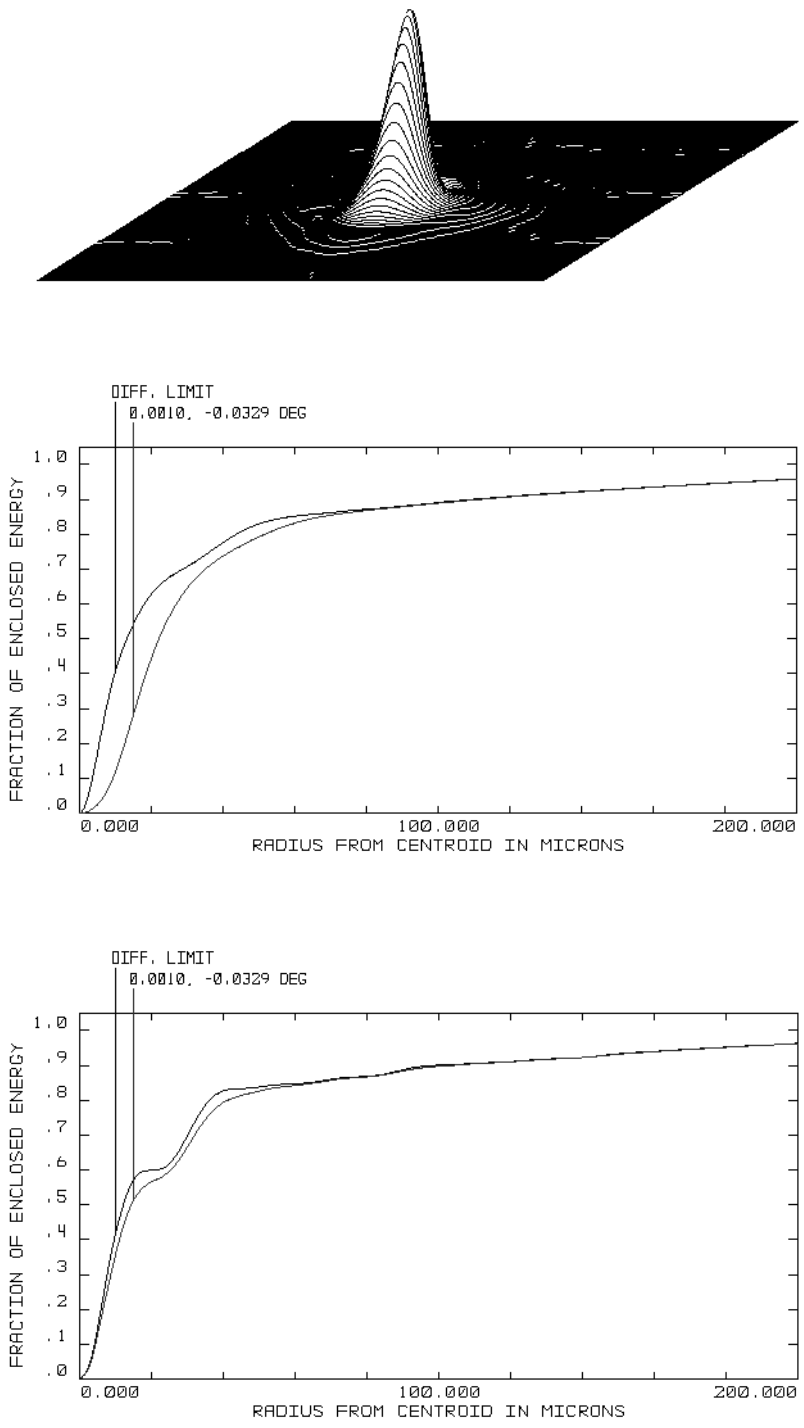

Figure 8: PSF for F300X at the edge of the field of view (top panel). Encircled energy for F300X at the edge of the field of view for a uniform spectrum (intermediate panel) and for a monochromatic source at the filter central wavelength (bottom panel)

It is clear from the figures that the finite filter widths degrade the PSF compared to what one would have for a monochromatic source at the effective wavelength of the filter. We have computed the values of sharpness at the center of the field of view and at the corner for each of these filters after pixelation (see Table 3). The values have been computed with perfect MTF. A residual field dependence is evident. This difference in sharpness from field center to the corner implies a difference in limiting magnitude of about 0.25 magnitudes for F218W, F225W, and F275W.

Filter	Center	Corner
F218W	0.2679	0.1867
F225W	0.2514	0.1570
F275W	0.1983	0.1453
F300X	0.0916	0.0872

Table 3. Values of the sharpness computed for the filters as designed and a flat input spectrum.

Clearly, for the broadest UV filter we should also expect a PSF dependence on the spectral energy distribution (SED) of the source being studied. In practice, the dominant effect is diffraction rather than focus. This is shown in Table 4 where we list the values of the sharpness for a PSF in F225W at the corner of the field of view for three different spectral energy distributions. Note that the center of the PSF moves by about half a pixel when going from the O star SED to the M star SED.

Source	Sharpness
O star	0.1566
Flat F_λ	0.1570
M star	0.1496

5. Conclusions

The presence of refractive elements in WFC3 UVIS would introduce a filter dependent defocussing if not corrected. This effect would be most significant in the UV where the refractive index of fused silica is varying most rapidly with wavelength. The filter effective thickness has been specified imposing a confocality condition so that this effect is corrected at the filter central wavelength. However, the finite bandwidth of our broad band filters leaves us with a residual effect which manifests itself as an overall degradation of

the PSF with a field dependence equivalent, for the UV broad band filters, to a loss of 0.25 magnitudes in limiting depth across the field of view .

6. Acknowledgement

I wish to thank Ray Boucarut (GSFC), Massimo Robberto (STScI), Joe Sullivan (Ball) and Michael Dittman (Ball) for useful discussions on various aspects of this problem.

7. References

JPL Specification Document D-18189 Version B, *Wide Field Camera 3 (WFC3) Optical filters*, JPL
Malitson, I.H. 1962, J. Opt. Soc. Am, 52, 1205